K_a distributions (also in Fig. 4) are slightly colder than the QCT calculations predict. However, they also peak at $K_a = 1$ and more closely resemble the QCT results on the T_1 surface than those calculated on S_0.

These five observations, common to both experiment and theory, appear contradictory to expectations. In particular, the very low rotational excitation accompanied by the consistently high vibrational excitation seems inconsistent with a reaction proceeding over a barrier. The important coordinate in this analysis is the HCO angle. At the T_1 transition state, this angle is much closer to free HCO than it is to the equilibrium bond angle on the T_1 surface (*13*, *19*). Therefore, this barrier might also be termed "late." This insight has been used previously (*12*) to infer that vibrationally excited HCO must arise from the S_0 channel, whereas distributions that are vibrationally and rotationally cold would indicate evolution of the reaction on the T_1 surface. Our experimental and QCT results call this assumption into question. In the QCT results, the reaction is guaranteed to evolve on the T_1 surface. Even so, the population in excited vibrational levels is substantial. This result can be explained in part by a sudden treatment of dynamics, which is appropriate for a barrier-dominated reaction. The CO bond length is roughly 0.015 Å longer at the saddle point than in HCO (*19*), and so vibrational excitation of the CO stretch is certainly plausible as a result. In addition, the T_1 saddle point geometry is nonplanar, with the departing H atom nearly perpendicular to the HCO plane. This geometry is probably the least efficient configuration for rotational excitation of the HCO fragment and may explain qualitatively why so little rotational excitation is seen.

In the experiments, both S_0 and T_1 states can contribute to the true population distributions. The agreement between the experimental and QCT distributions in Fig. 4 suggests very strongly that when formaldehyde is excited to these specific states, the triplet channel dominates. Clearly, population in excited vibrational states is not a fingerprint for the S_0 pathway. The most robust dynamical signature of the singlet channel is population in very high N and K_a states. The dynamical signature of the T_1 channel is high vibrational excitation coupled with very low rotational excitation.

The dynamical signatures of most of the formaldehyde chemical pathways have thus now been identified. Reaction on S_0 leads to statistical HCO, or to rotationally hot CO and vibrationally cold H_2, via the direct dissociation over the molecular channel saddle point; alternatively, rotationally cold CO and vibrationally hot H_2 can emerge via the roaming atom mechanism. Reaction on T_1 yields rotationally cold but vibrationally hot HCO. However, several notable issues remain to be addressed. One concerns the possibility of tunneling through the T_1 barrier. Experiment finds that

in region C, which is somewhat below the classical barrier height, the HCO rotational and vibrational distributions are similar to those in region D (above the barrier) rather than B (well below the barrier), suggesting that tunneling is present. Another, more general, issue is the electronic/nuclear coupling among the three electronic states, S_1, T_1, and S_0, which is clearly the next frontier to be explored.

References and Notes

1. G. P. Brasseur, J. L. Orlando, G. S. Tyndall, *Atmospheric Chemistry and Global Change* (Oxford Univ. Press, Oxford, 1999).
2. C. B. Moore, J. C. Weisshaar, *Annu. Rev. Phys. Chem.* **34**, 525 (1983).
3. The "roaming atom" channel involves trajectories that start out as a simple C-H bond cleavage; however, the H atom fails to escape because part of the available energy is tied up in other degrees of freedom (principally other HCO vibrations). The loosely bound H atom can roam around the periphery of the HCO moiety, where it encounters the other H atom, then behaves like an abstraction reaction and departs as H_2. This pathway involves a different region of the PES and results in completely different reaction dynamics (the CO is rotationally cold and the H_2 is vibrationally excited) than for the direct dissociation of the molecular products (an asymmetric planar transition state).
4. D. Townsend *et al.*, *Science* **306**, 1158 (2004).
5. M. J. H. Kemper, C. H. Hoeks, H. M. Buck, *J. Chem. Phys.* **74**, 5744 (1981).
6. X. Zhang, S. Zou, L. B. Harding, J. M. Bowman, *J. Phys. Chem. A* **108**, 8980 (2004).
7. A. C. Terentis, S. E. Waugh, G. F. Metha, S. H. Kable, *J. Chem. Phys.* **108**, 3187 (1998).
8. H.-M. Yin, K. Nauta, S. H. Kable, *J. Chem. Phys.* **122**, 194312 (2005).
9. X. Zhang, J. L. Rheinecker, J. M. Bowman, *J. Chem. Phys.* **122**, 114313 (2005).
10. M.-C. Chuang, M. F. Foltz, C. B. Moore, *J. Chem. Phys.* **87**, 3855 (1987).
11. M. J. Dulligan, M. F. Tuchler, J. Zhang, A. Kolessov, C. Wittig, *Chem. Phys. Lett.* **276**, 84 (1997).
12. L. R. Valachovic *et al.*, *J. Chem. Phys.* **112**, 2752 (2000).
13. Y. Yamaguchi, S. S. Wesolowski, T. J. van Huis, H. F. Schaefer III, *J. Chem. Phys.* **108**, 5281 (2002).
14. S. H. Lee, I. C. Chen, *J. Chem. Phys.* **103**, 104 (1995).
15. A. C. Terentis, S. H. Kable, *Chem. Phys. Lett.* **258**, 626 (1996).
16. The potential surface is a fit to roughly 20,000 UCCSD(T)/ aug-cc-pVTZ energies spanning the T_1 global minimum, the saddle point to the radical products, and the region beyond into the H + HCO channel. The energies were fit using the expression given in (*4*) and the root mean square fitting error is 95 cm^{-1} (0.27 kcal/mol) for energies up to 28 kcal/mol above the T_1 minimum, which is ~8 kcal/mol above the T_1 saddle point energy of the radical product channel. The electronic barrier to dissociation, H + HCO(e), is 2068 cm^{-1} (5.9 kcal/mol), which is quite close to the best ab initio value of 2130 cm^{-1} reported in (*14*).
17. MOLPRO is a package of ab initio programs written by H.-J. Werner and P. J. Knowles, with contributions from J. Almlof, R. D. Amos, A. Berning, D. L. Cooper, M. J. O. Deegan, A. J. Dobbyn, F. Eckert, S. T. Elbert, C. Hampel, R. Lindh, A. W. Lloyd, W. Meyer, A. Nicklass, K. Peterson, R. Pitzer, A. J. Stone, P. R. Taylor, M. E. Mura, P. Pulay, M. Schutz, H. Stoll, and T. Thorsteinsson.
18. Y.-T. Chang, C. Minichino, W. H. Miller, *J. Chem. Phys.* **96**, 4341 (1992).
19. J. M. Bowman, X. Zhang, *Phys. Chem. Chem. Phys.* **8**, 1 (2006).
20. S.H.K. and H.M.Y. thank the Australian Research Council for funding their research, and S. Rowling and A. Buell for assistance in the experiment and analysis. J.M.B. and X.Z. thank the U.S. Department of Energy (grant DE-FG02-97ER14782) for financial support and P. Zhang for useful discussions about the electronic structure calculations.

Late Precambrian Oxygenation; Inception of the Clay Mineral Factory

Martin Kennedy,[1]* Mary Droser,[1] Lawrence M. Mayer,[2] David Pevear,[1] David Mrofka[1]

An enigmatic stepwise increase in oxygen in the late Precambrian is widely considered a prerequisite for the expansion of animal life. Accumulation of oxygen requires organic matter burial in sediments, which is largely controlled by the sheltering or preservational effects of detrital clay minerals in modern marine continental margin depocenters. Here, we show mineralogical and geochemical evidence for an increase in clay mineral deposition in the Neoproterozoic that immediately predated the first metazoans. Today most clay minerals originate in biologically active soils, so initial expansion of a primitive land biota would greatly enhance production of pedogenic clay minerals (the "clay mineral factory"), leading to increased marine burial of organic carbon via mineral surface preservation.

Geochemical and physical evidence suggests that a stepwise increase in oxygen occurred around 1.1 to 0.54 billion years ago (Ga) (*1–5*) and was a necessary precondition to support the physiological needs of large metazoans (*6–8*). Whereas the dominant supply of free oxygen to the atmosphere is oxygenic photosynthesis, which began by at least 2.8 Ga (*9*), the changes in the earth system facilitating a rise in oxygen in the latest Precambrian remain controversial. Photosynthetic oxygen stays in the atmosphere and ocean unless it is consumed by

oxidation of organic matter or other reducing agents at the Earth's surface. The stepwise pattern of oxygen increase implies the modification or activation of a mechanism that became a permanent part of the oxygen and carbon cycles, one that should be important and apparent in modern

[1]Department of Earth Science, University of California Riverside, Riverside, CA 92521, USA. [2]Darling Marine Center, University of Maine, Walpole ME 04573, USA.

*To whom correspondence should be addressed. E-mail: martink@mail.ucr.edu

organic carbon burial but absent in the Pre-cambrian. Although many hypotheses have been offered to explain the late Precambrian rise of oxygen (1, 4, 8), the irreversible and stepwise pattern argues against processes that are epi-sodic, reversible, or equally active before and after the rise of oxygen, such as tectonics. Here, we offer a paradigm for organic carbon burial in Precambrian marine sediments based on clay minerals, the major cause of carbon preservation and burial in the modern system that we believe was initiated during the latest Precambrian.

Studies of modern marine systems over the past 10 years give a new understanding of how organic carbon enters the sedimentary record. Rather than the conventional model of particles of organic matter rapidly buried in sediment and preserved, the bulk of organic carbon deposited in continental margin sediments is dispersed among or bound to clay minerals (phyllosilicates), as indicated by strong correlations with surface area, data from physical separations, and microscopy (10–14). By contrast, discrete, unbound particu-late organic matter comprises <10% of total organic matter (TOC) (11, 13, 15). The spatial correlation of TOC with clay mineral concentra-tion is likely a result of a sheltering and preserv-ative effect that phyllosilicate surfaces provide to organic matter, and laboratory experiments show that mineral association powerfully enhances preservation of labile carbon compounds (15). Whatever the exact mechanism of protection, studies of both modern and ancient (16) sedi-ments indicate the first order importance of clays as a means of concentrating, accompany-ing, or preserving organic carbon (11, 13, 14).

Elemental and mineralogical trends indicate long-term changes in shale composition from the Precambrian to the Phanerozoic that could have important implications for an increase in clay production. There is a progressive decline in the K_2O/Al_2O_3 of shale (17, 18) in the Russian and the North American platforms. Loss of K relative to Al is expected with a shift from tektosilicate-dominated (feldspar and quartz) shales and siltstones, with minor amounts of illite-mica-chlorite accessory clays, to smectite- and kaolinite-dominated claystones [summarized in (18, 19); this trend is also influenced by burial diagenesis]. This chemical shift is consistent with a mineralogic shift from mica-illite and chlorite toward smectite, mixed layer smectite-illite, and kaolinite assemblages (19) typical of pedogenic clay minerals (PCM). Simultaneously, incom-pletely weathered arkose and greywacke become less abundant (18, 20), giving way to chemically mature orthoquartzite (21) (Fig. 1B).

On the basis of these data, we hypothesize secular change in the mineralogy of fine-grained marine sediments (shale and mudstone) from mechanically weathered micas and tektosilicates of high-temperature origin to a more phyllosilicate-rich pedogenic assemblage that should be associated with an enhanced preservation of organic carbon in the sedimentary reservoir in

the mode of modern sediments discussed above. The absence of a working Precambrian "clay factory" should be evident in the rock record, because PCM comprise an important sink of ions produced by weathering and, with recycled clays, make up >60% of Phanerozoic shale, the most common rock type at the Earth's surface (19).

To determine whether a secular change in clay abundance occurred during the latest Pre-cambrian, we investigated a prominent passive-margin succession spanning the 850 to 530 million years ago (Ma) transition in Australia. This succession was selected because it exhibited (i) a thick interval (>10 km) of passive-margin, shelfal, fine-grained, marine sediments, a major-ity of which are shales and mudstones (22) typical of depositional environments in which modern mudstones accumulate, and (ii) sufficient expo-sure to sample the finest-grained lithologies. Although the Australian section provides one of the most complete successions globally (it houses the stratotype section and point defining the Ediacaran Period) and is an ideal test of our hypothesis, we also studied successions in south China and Baltica. To avoid pitfalls of averaging, we sampled the finest-grained intervals within each succession (15 forma-tions total) (table S1) to test the hypothesis.

We found a striking increase in the x-ray diffraction (XRD) peak ratio of total phyllosili-

cates (clay minerals and micas) to quartz through the Neoproterozoic (Fig. 2) (23), supporting the hypothesis that clay formation increased radically at the end of the Proterozoic. We suggest that this trend most likely represents a secular change in PCM formation, delivery, and abundance rather than local, effects, diagenesis, or tectonically influenced trends, because it (i) occurs in multiple margins with different geologic histories, (ii) spans a broader range of time than any single process capable of influencing grain-size trends (i.e., sea level change, deltaic deposition, glacia-tion, etc.), and (iii) is robust across multiple depositional sequences (cycles of deepening) capable of concentrating the finest-grained frac-tion available. Additionally, there are no shale diagenetic mechanisms we are aware of that could account for such a strong shift from tektosilicates to octahedrally bound Al in phyllo-silicates in (pH neutral) marine sediments.

Because clay minerals deposited in marine sediments are sensitive records of continental paleoenvironments (24), a secular change in clay mineral abundance at the end of the Precambrian may have important implications for terrestrial soils. Unlike other detrital grains such as quartz or feldspar, most clay minerals are not produced by simple mechanical reduction of parent rock and should not be confused with mechanical reduction in grain size of any silicate to clay size
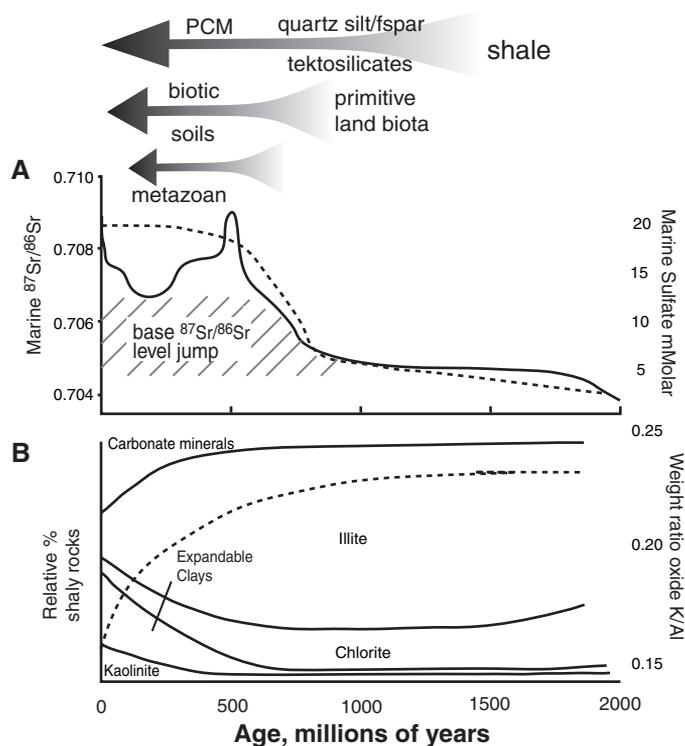
Fig. 1. (A) Solid line represents generalized $^{87}Sr/^{86}Sr$ seawater evo-lution from carbonate sediments [from (26)]. Minimum $^{87}Sr/^{86}Sr$ for a given age show a stepwise increase in $^{87}Sr/^{86}Sr$, suggested here to result from an increase in chemical weathering resulting from the advent of bio-genic soils. Dashed line represents the rise in concentration of dis-solved marine sulfate [from (2)], which coin-cides with general rise in atmospheric oxygen (2). (B) Solid lines and left axis record the increase in expandable clays and kaolinite (PCM) in-to the Phanerozoic rel-ative to illite, mica, and chlorite within shale from (19), reflecting illitization as well as enhanced chemical weathering and PCM production associated with biotic soils. The right axis and dashed line records K_2O/Al_2O_3 of shale from the North American and the Russian platforms compiled by (18), showing a shift toward PCM production from mechanically produced lithologies (mica, illite, and feldspar). Also see (17). Elemental data from our sample suite (table S1) show a positive relation between K and Al content (r = 0.614), suggesting postdepositional illitization is the dominant control on K/Al, but not necessarily on total clay, in the samples we studied.

(<2 μm). PCM rarely form by solid-state transformation of another mineral but rather precipitate as phyllosilicate crystals from cation-rich soil solutions that are in equilibrium with the ambient environment. Likewise, there is little evidence for large-scale conversion of tektosilicates (dominantly feldspars) to clay minerals in fine-grained sediments, and hydrothermal clay formation produces different clay mineral suites than those found in shales (*19*, *24*, *25*). The latitudinal mineralogical zoning of detrital clay minerals in modern marine sediments is consistent with increasing chemical weathering intensity with decreasing latitude, indicating the importance of this terrestrial contribution to marine clay deposition (*24*).

The lower clay mineral abundance in the earlier sections indicates a reduced continental chemical weathering intensity. This dilution does not, however, preclude the formation of clay minerals and their concentration in local depositional environments throughout the Proterozoic; such clay formation commonly occurs by weathering of volcanic sediments, and clay can be concentrated by sedimentary processes. However, it is not representative of the dominant mode of shale formation, and so these deposits should be rare. The increased phyllosilicates with time identify a new or enhanced source of PCM and increased clay sedimentation (apparent in Cambrian mudstones and through the Phanerozoic), whereas the increasing range of values indicates the effects on the growing clay flux by varying amounts of silt dilution. TOC (without considering sedimentation rate) does not record carbon burial flux; however,

TOC values (table S1) are at least consistent with our hypothesis, showing a commensurate rise with PCM even after thermal alteration.

Enhanced continental chemical weathering implied by PCM formation is also recorded in the step to more radiogenic $^{87}Sr/^{86}Sr$ values within Neoproterozoic seawater (*26*) (Fig. 1). Because the marine $^{87}Sr/^{86}Sr$ record provides a globally integrated measure of chemical weathering, it corroborates the secular origin for the clay mineral trend (Fig. 2). Seawater Sr isotopic composition derives from continental weathering and hydrothermal or mantle sources, whose contributions can be estimated because continental runoff is much richer in ^{87}Sr than hydrothermal sources. The Sr isotope record offers an important corroboration of the hypothesis because the seawater values can only be influenced by chemically weathered ions and will not change with variations in fluxes of mechanically weathered material (assuming constant hydrothermal contribution). Further, because minerals such as feldspar and mica derived from mechanical weathering of igneous and metamorphic rocks are strongly enriched in ^{87}Sr as well as K, an enhanced rate of chemical weathering and ion liberation to solution (and PCM formation) should increase $^{87}Sr/^{86}Sr$ in marine carbonates.

Two patterns of change mark the marine Sr isotopic record (Fig. 1): (i) a long-term (billion year) plateau with a major step at 0.7 Ga, establishing markedly more radiogenic marine values, and (ii) a shorter-term ($\sim$ 100 My) rise and fall in values coincident with the Cambrian Pan-African and the Tertiary Himalayan orogen-

ic events. Here we focus on the long-term, step-like rise of marine $^{87}Sr/^{86}Sr$ from 0.705 during the early Neoporoterozoic to 0.707, which begins in the late Neoproterozoic and subsequently comprises the lowest value through the Phanerozoic. We suggest that this new plateau results from an irreversible change in chemical weathering regime in parallel with a secular rise in clay mineral abundance.

What might have caused such a change in continental weathering? In the Phanerozoic, biotic soils promote production of PCM by providing organic matter that mechanically stabilizes soil profiles, retains cations and water, and increases fluid residence time (*24*, *27*). Whereas minor amounts of clay formation are possible directly on rock surfaces, the difficulties of retaining and concentrating leached ions are substantial, so that rock surfaces do not produce clay minerals as well as biotic soils. The biotic soil–forming environment for clay minerals can be likened to the carbonate "factory" within the carbonate system. In the absence of a clay mineral–forming mechanism before the late Precambrian, clay minerals deposited in marine sediments were probably not substantial until the evolution and colonization of the terrestrial environment by some form of a primitive land biota.

The transience of terrestrial environments (especially soils) prevents the geological record from preserving reliable evidence of the transformation from an abiotic to a biotic surface. However, physical and geochemical data suggest a primitive land biota by at least 1 Ga (*27*, *28*, *29*). Molecular evidence suggests mosses, fungi, and liverworts by $\sim$700 Ma (*30*) and a fossil marine fungi/lichen record by 600 Ma (*31*) [fungi markedly enhance weathering (*32*)]. Carbon isotopes of Neoproterozoic karst suggest that soil biomass was sufficient to impart a Phanerozoic-like meteoric isotopic signal to diagenetic carbonate (*31*). Thus although we cannot specifically identify the transitional states of a land biota, there is ample evidence for these transitions during the Proterozoic. Furthermore, modern microbial crusts stabilize soil profiles, retain water, enhance weathering rates, drive chemical differentiation, and provide chemically adsorptive organic matter (*32–34*). Thus, the advent of soils sufficiently biotic for clay formation likely predated complex terrestrial ecosystems (*33*, *35*).

One hypothesis for late Precambrian rise of oxygen calls on enhanced burial of organic matter associated with increased tectonic activity between 1.1 and 0.8 Ga (*4*). This hypothesis uses the positive relation between sedimentation rate and organic matter burial flux observed in modern sedimentary systems, which likely results from the scaling of clay mineral flux with total sedimentation rate (*13*). Our hypothesis changes the emphasis from temporal changes in quantity of deposition to changes in its quality, that is, its clay mineral abundance. The Neogene Bengal fan illustrates a variation on this theme.

Fig. 2. Secular changes in the relative amounts of phyllosilicate and quartz determined by using the Schultz ratio (*16*, *23*, *25*, *38*) for Neoproterozoic to Cambrian mudstones. Samples represent the finest-grained units that were at least 5 m thick from three locations: South Australia (triangles), Baltica (circles), and south China (squares). These data show an increase in the proportion of phyllosilicates relative to quartz with decreasing age. Because of the stability of quartz, its abundance serves as a crude
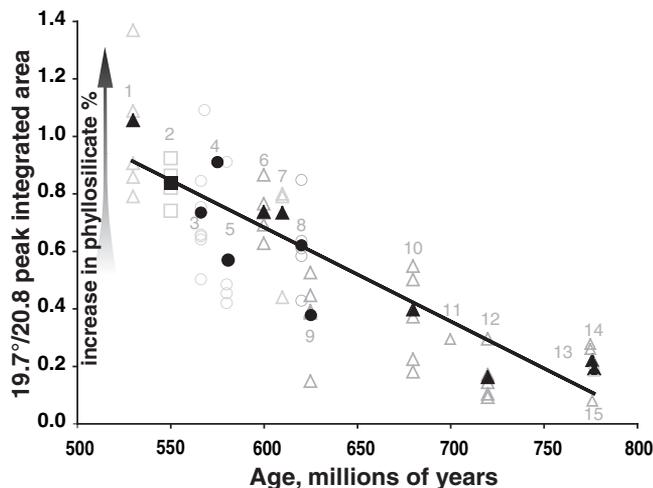
standard indicating the amount of tectosilicates either present (Schultz ratio low) or once present, now clay minerals (Schultz ratio high) in a shale of average chemical composition. Gray symbols are the range of values from a specific unit (all samples analyzed), whereas the solid figure is the average value for a given unit. Units studied include the following: 1, Oraparinna Shale; 2, Doushantuo Formation; 3, Birri Formation; 4, Ekre Shale; 5, Innerelva Member and Stappogiedde Formation; 6, Bunyeroo Formation; 7, Brachina Formation; 8, Nyborg Formation; 9, Reynella Member and Elatina Formation; 10, Enorama Shale; 11, Tarcowie Siltstone; 12, Tapley Hill Formation; 13, Mintaro Shale; 14, Saddleworth Formation; and 15, Woolshed Flat Shale. Age assignments are approximate, and correlations between basins have their basis in the assumed age of 630 Ma for the Marinoan (lower Varanger) glacial and 740 Ma for the Sturtian glacial. Sample locations, data, methods (including elemental data), and stratigraphic references can be found in table S1.

Onset of the monsoon in the Miocene drove an increase in chemical weathering in the Ganges-Brahmaprutra watersheds, resulting in a shift from mechanical weathering (tektosilicates, plus mica, illite, and chlorite) to chemical weathering (secondary detrital PCM; smectite, kaolinite) (36). The later PCM mineral assemblage resulted in an ~fourfold increase in organic loading and substantially increased the organic carbon burial flux (36).

The global change that promoted the rise of animals by 0.6 Ga (37) remains one of the most important yet least understood events in the geobiologic record. Here we adopt a non-uniformitarian approach by identifying an important component of the modern system that was largely absent or ineffective in the Precambrian and changed in an irreversible manner sometime during the Neoproterozoic. The modern ocean buries 1.6×10^{14} g C/year, of which 86% (1.38×10^{14} g C/year) is buried in ocean margins (11), where OC concentration and hence burial flux is linearly proportional to clay content. Applying this burial rate throughout the Phanerozoic and assuming that the peak ratios in Fig. 2 are proportional to clay content, then the clay-driven increase in OC burial that developed during 730 to 500 Ma (Fig. 2) ramped from 0.21×10^{14} to 1.38×10^{14} g C/year. The resulting sixfold increase in oxygen retention would have greatly influenced biogeochemical cycling of redox sensitive elements such as Fe^{+2} and S^{2-} (2, 3, 5) and ultimately increased the oxygen concentration of the atmosphere. The evolutionary innovation and expansion of land biota could permanently increase weathering intensity and PCM formation, establishing a new level of organic carbon burial and oxygen accumulation.

References and Notes

1. L. A. Derry, A. J. Kaufman, S. B. Jacobsen, *Geochim. Cosmochim. Acta* **56**, 1317 (1992).
2. L. C. Kah, T. W. Lyons, T. D. Frank, *Nature* **431**, 834 (2004).
3. D. E. Canfield, A. Teske, *Nature* **382**, 127 (1996).
4. D. J. Des Marais, H. Strauss, R. E. Summons, J. M. Hayes, *Nature* **359**, 605 (1992).
5. S. T. Brennan, T. K. Lowenstein, J. Horita, *Geology* **32**, 473 (2004).
6. P. Cloud, *Paleobiology* **2**, 351 (1976).
7. B. Runnegar, *Alcheringa* **6**, 223 (1982).
8. A. H. Knoll, *Life on a Young Planet* (Princeton Univ. Press, Princeton, NJ, 2003), p. 247.
9. J. Brocks, G. A. Logan, R. Buick, R. E. Summons, *Science* **285**, 1033 (1999).
10. R. G. Keil, E. Tsamakis, C. B. Fuh, J. C. Giddings, J. I. Hedges, *Geochim. Cosmochim. Acta* **58**, 879 (1994).
11. J. I. Hedges, R. G. Keil, *Mar. Chem.* **49**, 81 (1995).
12. L. M. Mayer, L. L. Schick, K. R. Hardy, R. Wagai, J. McCarthy, *Geochim. Cosmochim. Acta* **68**, 3863 (2004).
13. L. M. Mayer, *Geochim. Cosmochim. Acta* **58**, 1271 (1994).
14. B. Ransom, K. Dongseon, M. Kastner, S. Wainwright, *Geochim. Cosmochim. Acta* **62**, 1329 (1998).
15. R. G. Keil, D. B. Montlucon, F. G. Prahl, J. I. Hedges, *Nature* **370**, 549 (1994).
16. M. J. Kennedy, D. R. Pevear, R. J. Hill, *Science* **295**, 657 (2002).
17. R. Cox, D. R. Lowe, R. L. Cullers, *Geochim. Cosmochim. Acta* **59**, 2919 (1995).
18. R. M. Garrels, F. T. Mackenzie, *Evolution of Sedimentary Rocks* (Norton, New York, 1971), p. 397.
19. C. E. Weaver, *Clays, Muds and Shales* (Developments in Sedimentology, Elsevier, New York, 1989), p. 819.
20. A. B. Ronov, *Geokhimiya* **8**, 715 (1964).
21. R. H. Dott Jr., *J. Geol.* **111**, 387 (2003).
22. W. V. Preiss, *Bull. Geol. Surv. S. Australia* **53**, 438 (1987).
23. The Schultz ratio is an uncalibrated, dimensionless number that specifically indicates the relative amount of total phyllosilicates versus quartz by using the x-ray peak intensities for the sum of all phyllosilicates (020 peak, 19.8° 2 Θ, Cu Ka radiation) and quartz (100 peak, 20.8° 2Θ) on random powder mounts. For a granite or clean sandstone, this number would be <0.2. For mudstones and pelitic metamorphics (clay shales, mudstones, slates, and mica schists), it typically is between 0.2 and 2.0. Sediment derived from fine grinding of granite to clay size does not change the Schultz ratio unless dissolution and reprecipitation as a clay mineral has occurred. It is an indicator of available clay minerals in the provenance area, both recycled, and newly formed by soil processes. Later clay diagenesis (such as illitization) does not change the Schultz ratio because it typically converts one phyllosilicate to another.
24. H. Chamley, *Clay Sedimentology* (Springer, Berlin, 1989), p. 623.
25. L. G. Schultz, *U. S. Geol. Surv. Tech. Rep. No. 391C* (1964).
26. G. Shields, J. Veizer, *Geochem. Geophys. Geosystems* **3**, 1 (2002).
27. G. J. Retallack, *Soils of the Past, an Introduction to Pedology* (Blackwell Science, Oxford, ed. second, 2001), p. 404.
28. A. R. Prave, *Geology* **30**, 811 (2002).
29. R. J. Horodyski, L. P. Knauth, *Science* **263**, 494 (1994).
30. D. S. Heckman *et al.*, *Science* **293**, 1129 (2001).
31. X. Yuan, S. Xiao, T. N. Taylor, *Science* **308**, 1017 (2005).
32. A. Neaman, J. Chorover, S. L. Brantley, *Am. J. Sci.* **305**, 147 (2005).
33. S. E. Campbell, *Origins Life* **9**, 335 (1979).
34. J. F. Banfield, W. W. Barker, S. A. Welch, A. Taunton, J. V. Smith, *Proc. Natl. Acad. Sci. U.S.A.* **96**, 3404 (1999).
35. J. A. Raven, D. Edwards, *J. Exp. Bot.* **52**, 381 (2001).
36. C. France-Lanord, L. A. Derry, *Nature* **390**, 65 (1997).
37. A. H. Knoll, S. B. Carroll, *Science* **284**, 2129 (1999).
38. F. L. Lynch, *Clays Clay Miner.* **45**, 618 (1997).
39. We thank S. Jensen, T. Bristow, G. Jiang, J. Gehling, and M. Fuller for help in the field. This work was sponsored by NASA grant NWG04GJ42G and NSF-EAR grants 0223198 and 0345207.

The Last Deglaciation of the Southeastern Sector of the Scandinavian Ice Sheet

V. R. Rinterknecht,[1]*† P. U. Clark,[1] G. M. Raisbeck,[2] F. Yiou,[2] A. Bitinas,[3] E. J. Brook,[1] L. Marks,[4] V. Zelčs,[5] J.-P. Lunkka,[6] I. E. Pavlovskaya,[7] J. A. Piotrowski,[8] A. Raukas[9]

The Scandinavian Ice Sheet (SIS) was an important component of the global ice sheet system during the last glaciation, but the timing of its growth to or retreat from its maximum extent remains poorly known. We used 115 cosmogenic beryllium-10 ages and 70 radiocarbon ages to constrain the timing of three substantial ice-margin fluctuations of the SIS between 25,000 and 12,000 years before the present. The age of initial deglaciation indicates that the SIS may have contributed to an abrupt rise in global sea level. Subsequent ice-margin fluctuations identify opposite mass-balance responses to North Atlantic climate change, indicating differing ice-sheet sensitivities to mean climate state.

At its maximum extent, the Scandinavian Ice Sheet (SIS) merged with the Barents Ice Sheet (BIS) and Kara Ice Sheet to form a Eurasian ice sheet complex that was the second largest of the former Northern Hemisphere ice sheets (1–3). Such a large ice mass would have influenced climate on scales ranging from regional to hemispheric and may have affected the formation of North Atlantic deep-water through releases of meltwater and icebergs. Simulations with climate models suggest that the mass balance of the SIS was particularly sensitive to changes in North Atlantic climate because of its location immediately downwind of the North Atlantic Ocean (4). Finally, the SIS deformed the underlying crust, and the record of postglacial isostatic recovery can be inverted to reveal geophysical properties of the lithosphere and mantle (5, 6).

Isolating the relative contributions of the SIS to changes in global sea level, climate, and the solid Earth requires that the chronology of its growth and decay be well constrained. Ice-

[1]Department of Geosciences, Oregon State University, Corvallis, OR 97331, USA. [2]Centre de Spectrométrie Nucléaire et de Spectrométrie de Masse, 91405 Orsay, France. [3]Geological Survey of Lithuania, LT-03123 Vilnius, Lithuania. [4]Polish Geological Institute, 00-975 Warsaw, Poland. [5]Department of Geography and Earth Sciences, University of Latvia, Riga, LV-1586, Latvia. [6]Institute of Geosciences, University of Oulu, Post Office Box 3000, Linnanmaa 90014, Finland. [7]National Academy of Sciences of Belarus, Institute of Geological Sciences, 220141 Minsk, Belarus. [8]Department of Earth Sciences, University of Aarhus, DK-8000 Aarhus, Denmark. [9]Institute of Geology, Tallinn University of Technology, 10143 Tallinn, Estonia.

*Present address: Lamont-Doherty Earth Observatory, Columbia University, Palisades, NY 10964, USA.
†To whom correspondence should be addressed. E-mail: vincent@ldeo.columbia.edu